Synchronization mechanism and optimization of spreading sequences in chaos-based DS-CDMA systems

PAPER *Special Section on Nonlinear Theory and Its Applications*

Synchronization Mechanism and Optimization of Spreading Sequences in Chaos-Based DS-CDMA Systems*

Gianluca SETTI[†], **Riccardo ROVATTI**[††], *and* **Gianluca MAZZINI**[†], *Nonmembers*

SUMMARY The aim of this contribution is to take a further step in the study of the impact of chaos-based techniques on classical DS-CDMA systems. The problem addressed here is the sequence phase acquisition and tracking which is needed to synchronize the spreading and despreading sequences of each link. An acquisition mechanism is considered and analyzed in depth to identify analytical expressions of suitable system performance parameters, namely outage probability, link startup delay and expected time to service. Special chaotic maps are considered to show that the choice of spreading sequences can be optimized to accelerate and improve the spreading codes acquisition phase.

key words: *chaos-based DS-CDMA systems, acquisition and tracking, Markov chains*

1. Introduction

The idea of using signals produced by chaotic systems in the communication field is primarily linked to their broad-band noise-like nature. In fact, as a consequence of the well-known sensitivity of initial conditions, signals generated by chaotic systems are characterized by rapidly vanishing cross- and auto-correlation functions.

Two ways of exploiting this peculiar feature in digital signals transmission have been proposed so far.

In the first way, following a modulation-oriented approach, the main idea is to map information symbols on slices of chaotic (and thus non-periodic and wide-band) signals instead of transmitting periodic waveforms. The expected benefits rely on the fact that the cross-correlation between segments of a chaotic waveform is lower than between pieces of periodic signals. Hence, chaos-based modulation techniques can potentially offer better performance in extremely noisy environments and under multipath propagating conditions [1], [2]. Though these positive features are balanced by the problem of determining a method to effectively demodulate chaos-carried signals [3], noteworthy development are being achieved in this field [4], [5].

In the second way, referring to a different system-oriented approach, chaotic signals are exploited to improve the performance of existing communication systems based on statistical properties of the transmitted symbols. In particular, increasing attention has been paid to the generation of spreading sequences for a standard DS-CDMA system by means of chaotic time series. For instance, in [6] some simulation based comparisons between Gold sequences and those generated using chaotic time series are reported for a synchronous system while in [7], the problem is addressed for the much more difficult asynchronous case and numerical computations of even- and odd-correlation functions are given for the Chebyshev map.

Recently, encouraging theoretical and practical results have been obtained for an asynchronous DS-CDMA environment [8]–[10]. When sequences constructed by truncating and repeating a chaotic time series are employed, an analytical estimation of the asynchronous co-channel interference has been obtained by means of advanced tools from statistical dynamical systems theory. With this, the viability of the chaos-based approach for the improvement of existing DS-CDMA systems can be demonstrated along at least two directions. First, chaotic generation of spreading sequences is not subject to the impairing limitations in terms of number of users and allocated spreading factor which is characteristic of shift-register generated sequences. Second, chaotic systems exist that can be exploited to generate spreading sequences that outperform classical ones in terms of co-channel interference reduction.

Aim of this contribution is to evaluate the impact of the adoption of chaos-based spreading on the procedure of sequence phase acquisition and tracking which is needed to synchronize the transmitted spreading sequences with those used for demodulation. This problem is, in general, quite difficult as it implies joint synchronization between carrier phases, spreading sequence timing, and spreading sequence integer shift. Since the choice of different sets of spreading sequences mainly affects the last aspect, we here discuss an improved version of the acquisition mechanism proposed in [12]. Adopting this algorithm, some efficiency indexes can be defined and used as a mean to evaluate system performance from a synchronization point of view when chaos-based spreading sequences are employed. To obtain the analytical expression of these performance merit figures, a general method is developed to derive the steady-state probability of systems whose states are characterized by a given distribution

Manuscript received December 5, 1998.

[†]The authors are with D.I., University of Ferrara, via Saragat 1, 44100 Ferrara, Italy.

[††]The author is with D.E.I.S., University of Bologna, viale Risorgimento 2, 40136 Bologna, Italy.

*Part of this paper was presented at the International Symposium on Nonlinear Theory and its Applications (NOLTA'98).

of sojourn times and are linked with each other by a transition graph.

Moreover, since many chaotic maps qualify as good candidates for sequence generations [8], [9], it can be expected that a proper optimization phase may lead to further performance improvements. Therefore, in this paper, some new one-dimensional chaotic systems are constructed which can be effectively used for sequence generation. As a result of this optimization effort, examples of chaos-based spreading sequences outperforming classical ones (m- and Gold sequences) in synchronization can be determined.

The paper is structured as follows. First, the synchronization mechanism is reviewed along with the analytical expressions of efficiency indexes [12]. The expression of some of these indexes depend on a Theorem for the analysis of general finite-state systems which is reported in the Appendix. After this, the results of a first optimization effort are reported: different chaotic systems are tried and sequence generation is repeated many times to achieve the maximum reduction in terms of expected start up delay and expected time to service. Numerical results for these optimal sequence sets are reported showing the possibility of achieving a further improvement with respect to previously reported results [12].

2. Synchronization Mechanism for DS-CDMA Systems

Consider a baseband equivalent scheme of a classical asynchronous DS-CDMA system [8], for which a common carrier with pulsation ω_0 is assumed, U users are supposed and where the absolute delay t^u and the corresponding carrier phase θ^u, $u = 1, 2, \ldots, U$, must be considered to vary randomly from user to user. From the u-th useful user viewpoint, the simplified baseband scheme can be represented as shown in Fig. 1, where $S^u(t) = \sum_{s=-\infty}^{\infty} S_s^u g_T(t - sT)$ is the PAM information signal with information symbols $S_s^u \in \{-1, +1\}$, g_T represents a rectangular pulse equal to 1 within $[0, T]$ and 0 outside, and a normalized unitary peak amplitude is assumed. This signal is spread by the complex PAM signal $q^u(t)$, formed by rectangular pulses $g_{T_{\text{chip}}}$ whose symbol frequency $1/T_{\text{chip}}$ is N times the symbol frequency of $S^u(t)$ and which is modulated by the spreading code symbols x_s^u of the alphabet X which are mapped into the complex L-th roots of 1 in $Z = \{z_1, \ldots, z_L\} \subset \mathbb{C}$ by means of a function $Q : X \mapsto Z$. The spreading signal acting on the information stream of the u-th user is $q^u(t)e^{\imath\theta^u}$ where $\imath$ is the imaginary unit and a quadrature modulator with carrier phase θ^u is employed.

The resulting signal is transmitted over a channel in which thermal noise and interference from the other $U - 1$ users are added. The corrupted signal is then despread multiplying it by $q^u(t + \Delta t)$ and feeding the result into an integrate-and-dump stage. In order to achieve correct symbol demodulation Δt must be zero. The mechanism proposed here is able to achieve this phase synchronization assuming that all the time shifts are integer multiple of T_{chip} and controlling a local shift $\Delta t'$ which is substracted to the delay due to transmission $\Delta t''$ to obtain $\Delta t = \Delta t'' - \Delta t' = \tau T_{\text{chip}}$. With this, $\tau = 0$ when the delay between the transmitter spreading sequence and the receiver despreading sequence are matched.

From the synchronization mechanism point of view, the link of each user works at any given time in one of three different modes as shown in Fig. 2. In Idle mode (I) the spreading and despreading sequence are not synchronized, no reliable communication is possible even if the system is trying to achieve it. In Acquisition mode (A) the two sequences are synchronized and the system is verifying the link availability. In Service mode (S) communication is possible.

With this, several parameters can be defined describing the system behavior from a synchronization viewpoint. In fact, at each given time the link has a probability Π_{o} of being not in service mode, which will be referred to as *outage probability*. Moreover, if the link cannot provide the service at that time, a certain delay must be suffered before communication can start. We will measure this *link start up delay* as an integer multiple of T_{chip} and indicate its expected value as T_{ac}. Finally, we may also consider the product $\Xi = T_{\text{ac}}\Pi_{\text{o}}$

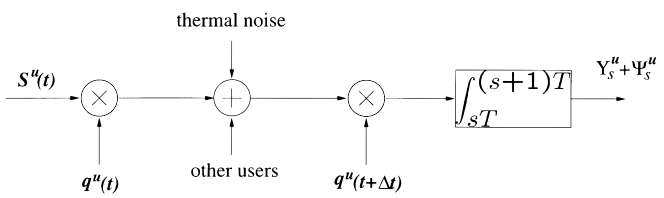

Fig. 1 Communication link from the point of view of the useful u-th user.

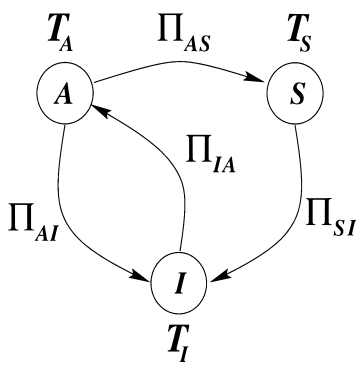

Fig. 2 Three-mode model of CDMA communication link: S means link is in service, A means link is active but not in service, I means link is idle. T_S, T_A and T_I represent the expected time the system remains in each mode, and Π_{ij} are the associated transition probabilities.

which can be thought of as the *expected time* a generic u-th user must wait *before the link is able to provide service*.

More in detail, the acquisition and tracking mechanism we analyze is a suitable generalization of a classical one [11] and can be described by means of a Markov chain. Each state is associated with an integer offset τ between the spreading sequence at the transmitter and the receiver side.

In each state the despreading sequence is shifted by the appropriate offset, multiplied by the incoming signal and fed into the integrate-and-dump, whose output, corresponding to the s-th information symbol, is made of two components Ψ_s^u and Υ_s^u, as shown in Fig. 1. The first component Ψ_s^u accounts for the interference of the other $U-1$ users and has been thoroughly characterized in [8] and [9]. The second component Υ_s^u accounts for the despreading of a shifted version of the useful signal and can be expressed as [15]

$$\Upsilon_s^u = S_{s-1}^u \,\mathrm{Re}[\Gamma_{N,N-\tau}] + S_s^u \,\mathrm{Re}[\Gamma_{N,\tau}]$$

where the partial auto-correlation function

$$\Gamma_{N,\tau} = \begin{cases} \dfrac{1}{N}\displaystyle\sum_{k=0}^{N-\tau-1} Q(x_k^u)Q^*(x_{k+\tau}^u) & 0 \le \tau < N \\ \Gamma_{N,-\tau}^* & -N < \tau < 0 \\ 0 & |\tau| \ge N. \end{cases} \tag{1}$$

accounts for the multiplication by the shifted despreading sequence and the subsequent integration [8].

The modulus of the output of this stage is then compared against a suitable threshold α. This comparison discriminates between high values of the output (which are presumably generated by synchronized despreading) and low values (which should indicate not properly synchronized situations).

Before declaring synchronization a number κ of consecutive above-threshold outputs are required [14]. Once synchronization has been claimed, a tracking mechanism checks the same signal and revokes synchronization whenever more than η consecutive correlate-and-dump outputs are not greater than α. This prevents the system from getting stuck in a non-synchronized status although creating a non-negligible probability of leaving the true synchronized state.

The chain is started from one of the N states $\mathbf{X}_0, \ldots, \mathbf{X}_{N-1}$. Whenever synchronization cannot be claimed, the subsequent integer shift is tried setting $\tau \leftarrow (\tau+1)_{\mathrm{mod}\, N}$ and going to the corresponding state $\mathbf{X}_{(\tau+1)_{\mathrm{mod}\, N}}$.

A more formal description of this strategy can be given in terms of the state diagram reported in Fig. 3. Testing the integrate-and-dump output, the automata follows either the $|\Upsilon_s^u + \Psi_s^u| > \alpha$ or the $|\Upsilon_s^u + \Psi_s^u| \le \alpha$ branch out of each state. The overall behavior is non-deterministic as co-channel interference and thermal noise affect the observed signal and each branch is characterized by a probability of being taken. Following [8], [11] we will assume that the probability of obtaining an above-threshold value when synchronized ($\tau = 0$) can be defined and computed as

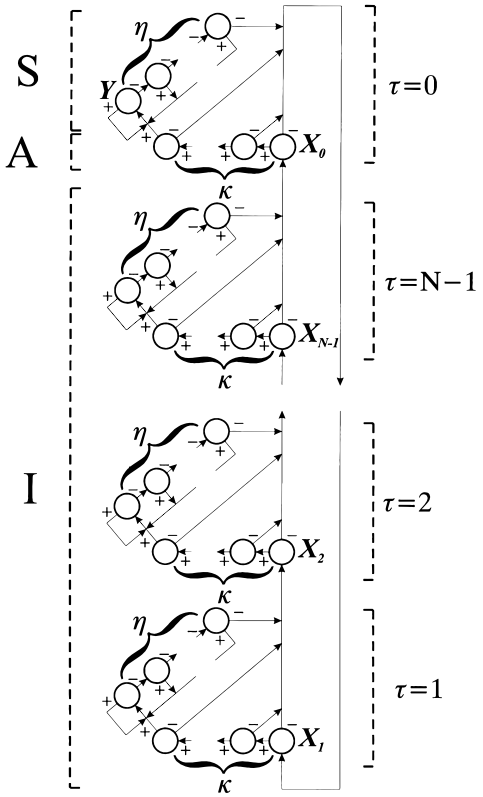

Fig. 3 Overall state diagram of the synchronization strategy: + branches are taken when the modulus of $\Upsilon_s^u + \Psi_s^u$ is greater than α while − branches are taken when the modulus of $\Upsilon_s^u + \Psi_s^u$ is less than or equal to α.

$$P_D = \Pr\{|\Omega_s^u + \Psi_s^u| > \alpha\}$$

where Ω_s^u is the value of Υ_s^u with $\tau = 0$.

When the system is in a non-synchronized state ($\tau \neq 0$), $\Upsilon_s^u + \Psi_s^u$ can be thought as a random variable depending also on S_{s-1}^u, S_s^u, τ and on the spreading sequence. Hence, non-synchronization appears as a self-interference term affecting the decoder output and thus the probability of obtaining an above-threshold value when not synchronized. In the following we will assume that such an event can be represented by a single, average, probability [8]

$$P_F = \frac{1}{N-1}\sum_{\tau=1}^{N-1} \mathbf{E}_{S_{s-1}^u, S_s^u}[\Pr\{|\Upsilon_s^u + \Psi_s^u| > \alpha\}]$$

so that the statistical feature of Υ_s^u directly affect the performance of the synchronization mechanisms. Such an influence has been investigated by extensive simulation in [12], while in [15], [16] it has been shown that Υ_s^u can be effectively approximated with a continuous

Gaussian random variable, by evaluating its moments $\mathbf{E}[(\Upsilon_s^u)^m]$, $m = 0, 1, 2, \ldots$, which result to be close to those of a Gaussian random variable for typical values of N.

In Fig. 3, the parts of the non-deterministic automata corresponding to the three modes S, A and I of the link (Fig. 2) are highlighted. From this representation it can be easily seen that the estimation of $T_{\rm ac}$ depends on the estimation of the time required to discard a $\tau \neq 0$ and try the subsequent shift $(\tau+1)_{\bmod N}$.

This estimation can be carried out exploiting the well-known properties of the z-transform for the analysis of discrete-time systems. In particular, the transfer function between the states $\mathbf{X}_\tau$ ($\tau \neq 0$) and $\mathbf{X}_{\tau+1}$ corresponding to two subsequent shifts is

$$\begin{aligned} H(z) &= \sum_{i=0}^{\kappa-1}(1-P_F)z(P_F z)^i + (P_F z)^\kappa A_\eta^{P_F}(z) \\ &= (1-P_F)z\frac{1-P_F^\kappa z^\kappa}{1-P_F z} + P_F^\kappa z^\kappa A_\eta^{P_F}(z) \end{aligned} \qquad (2)$$

where $A_\eta^{P_F}(z)$ accounts for the looping part of the transfer function and can be derived considering the induction $A_0^p(z) = 1$ and $A_{k+1}^p(z) = A_k^p(z)(1-p)z/(1 - A_k^p(z)pz)$, which can be unrolled to give

$$A_\eta^{P_F}(z) = \frac{(1-P_F)^\eta z^\eta (1-z+P_F z)}{1-z+z^{\eta+1}(1-P_F)^\eta P_F}$$

According to the proposed mechanism, once that $\tau = 0$ is reached, $\Omega_s^u + \Psi_s^u$ is checked κ times so that the transfer function between state $\mathbf{X}_0$, which is the first associated with $\tau = 0$, and state $\mathbf{Y}$, which is the first ensuring the S mode for the link, is $O(z) = (P_D z)^\kappa$.

If, despite $\tau = 0$, co-channel interference and thermal noise cause the integrate-and-dump output to be not greater than α at one of these κ steps, synchronization is not recognized so that a non-null transfer function from $\mathbf{X}_0$ to $\mathbf{X}_1$ exists in the form

$$\begin{aligned} F(z) &= (1-P_D)z\sum_{i=0}^{\kappa-1}(P_D z)^i \\ &= (1-P_D)z\frac{1-(P_D z)^\kappa}{1-P_D z} \end{aligned}$$

Assume now that the synchronization mechanism is run starting from a random uniformly distributed τ. The transfer function between $\mathbf{X}_\tau$ and $\mathbf{Y}$ can, again, be derived from Fig. 3, to be

$$\begin{aligned} U_\tau(z) &= O(z)H^{(N-\tau)_{\bmod N}}\sum_{i=0}^{\infty}(F(z)H^{N-1}(z))^i \\ &= \frac{O(z)H^{(N-\tau)_{\bmod N}}}{1-F(z)H^{N-1}(z)} \end{aligned}$$

With this we may now recall that the expected time needed to go from $\mathbf{X}_\tau$ to $\mathbf{Y}$ is $\lim_{z\to 1}\frac{\partial U_\tau}{\partial z}(z)$ so that, for uniformly distributed starting shifts the expected acquisition time is

$$\begin{aligned} T_{\rm ac} &= \frac{1}{N}\sum_{\tau=0}^{N-1}\lim_{z\to 1}\frac{\partial U_\tau}{\partial z}(z) \\ &= \lim_{z\to 1}\left\{\frac{O(z)\left[\frac{\partial F}{\partial z}(z) + (N-1)F(z)\frac{\partial H}{\partial z}(z)\right]}{[1-F(z)]^2}\right. \\ &\quad \left. + \frac{2\frac{\partial O}{\partial z}(z) + (N-1)O(z)\frac{\partial H}{\partial z}(z)}{2[1-F(z)]}\right\} \end{aligned}$$

Note that $T_{\rm ac}$ is a function of P_F and P_D which, in turn, account for co-channel interference and thermal noise. In the ideal case, when no interference or noise are present, we have $P_F \to 0$ and $P_D \to 1$ and simple calculations lead to $T_{\rm ac} \to \frac{N-1}{2} + \kappa$ which corresponds to the intuitive idea that, on the average, synchronization is achieved after trying half of the possible shifts and waiting for the final κ-steps validation.

With the aid of Fig. 3 and its decomposition into the three link modes, it is also possible to derive the expected permanency in each of them. Namely

$$\begin{aligned} T_A &= \sum_{i=0}^{\kappa-1}(i+1)(1-P_D)P_D^i + \kappa P_D^\kappa \\ &= \frac{1-P_D^\kappa}{1-P_D} \\ T_I &= \lim_{z\to 1}\frac{\partial H^{N-1}}{\partial z}(z) \\ &= (N-1)\left[\frac{1-P_F^\kappa}{1-P_F} + P_F^\kappa\frac{1-(1-P_F)^\eta}{P_F(1-P_F)^\eta}\right] \\ T_S &= \lim_{z\to 1}\frac{\partial A_\eta^{P_D}}{\partial z}(z) = \frac{1-(1-P_D)^\eta}{P_D(1-P_D)^\eta} \end{aligned}$$

To derive the steady-state outage probability $\Pi_{\rm o}$ let us now consider the asymptotic behavior of the three-modes scheme in Fig. 2. Once that the system exits an operating mode, it may fall into the others with a certain probability. These probabilities can be arranged in the transition matrix

$$\bar{\Pi} = \begin{bmatrix} 0 & 0 & P_D^\kappa \\ 1 & 0 & 1-P_D^\kappa \\ 0 & 1 & 0 \end{bmatrix}$$

which is non-negative and irreducible [13] so that a unique eigenvector $\pi = [\pi_S\ \pi_I\ \pi_A]$ exists corresponding to the unit eigenvalue. Few easy computations give

$$\pi_A = \pi_I = 1 \quad \pi_S = P_D^\kappa$$

Exploiting the Theorem proved in the Appendix we may use Eq. (A·7) to compute the outage probability as

$$\Pi_o = 1 - \Sigma_S = 1 - \frac{\pi_S T_S}{\pi_S T_S + \pi_A T_A + \pi_I T_I}$$

It is worthwhile to stress that this expression can be evaluated in the ideal no-interference and noiseless case ($P_D \to 1$, $P_F \to 0$) to give $\pi_S \to 1$, and $T_A \to \kappa$, $T_I \to N-1$, $T_S \to \infty$, so that $\Pi_o \to 0$ as one could coherently expect.

3. Numerical Results and Optimization

To highlight the differences in the system behavior when classical and chaos-based spreading sequences are employed, we report in this section the numerical evaluation of the performance parameters computed in Sect. 2.

More in detail, we refer to the case of a system with a number of users $U \leq U_{\max} = 30$ and assume the spreading factor N to be fixed at a typical value of 70. Moreover, the influence of thermal noise is not considered to emphasize the role of different spreading sequences on the system performance.

We consider classical m-sequences and Gold sequences with a number of levels L equal to 2, 3 and 5. In order to obtain a spreading factor of 70 and to allocate 30 users, we choose $m = 9, 6, 4$ when $L = 2, 3, 5$ respectively for m-sequences, while $m = 7, 5, 3$ when $L = 2, 3, 5$ for Gold sequences. Sequences longer than the spreading factor are shortened by truncation [17].

The chaos-based sequences taken into consideration are generated by four different maps, a n-way Bernoulli Shift (BS, with $n = 10$), a n-way Tailed Shift (TS, with $n = 10$), whose general properties are discussed in detail in [8], [9] and two other piecewise affine Markov maps. The first of these two maps will be indicated as Map 1 and is a slight modification of the 10-way Tailed Shift with two tails. The second map will be indicated as Map 2 and is a slight modification of a 10-way Bernoulli Shift in which the central ways have a unit slope and the slope of the other ways is adjusted to maintain a unit invariant probability density.

In Figs. 4, 5 and 6 we assume $U = 15$ and $L = 2, 3$, and we report the dependency of the expected delay to service Ξ on each of the three parameters α, κ, η, while the other two are kept constant. As it can be noticed, chaotic maps exist, whose generated sequences offer better performance with respect to the classical ones, and sequences generated by means of Map 2 always give rise to the best results.

As far as initial condition optimization is concerned, the results shown in Figs. 7, and 8 have been achieved considering the sequences resulting in the best performance values in 100 trials. It is worthwhile to stress, that the optimization phase has been carried out referring to the maximum number $U_{\max}$ of users allowed in the channel. Of course, this is not the only possible choice, since a separate optimization could be performed for every value of $U \leq U_{\max}$, potentially obtaining better performance. Yet, in this case, whenever the communication load varies of even a single unit, a change of the sequences is needed for all users. This procedure would induce a potentially long outage of all the active links for system reconfiguration and resynchronization. Moreover, triggering and controlling this process would require a dedicated link, which would increase the overall system complexity.

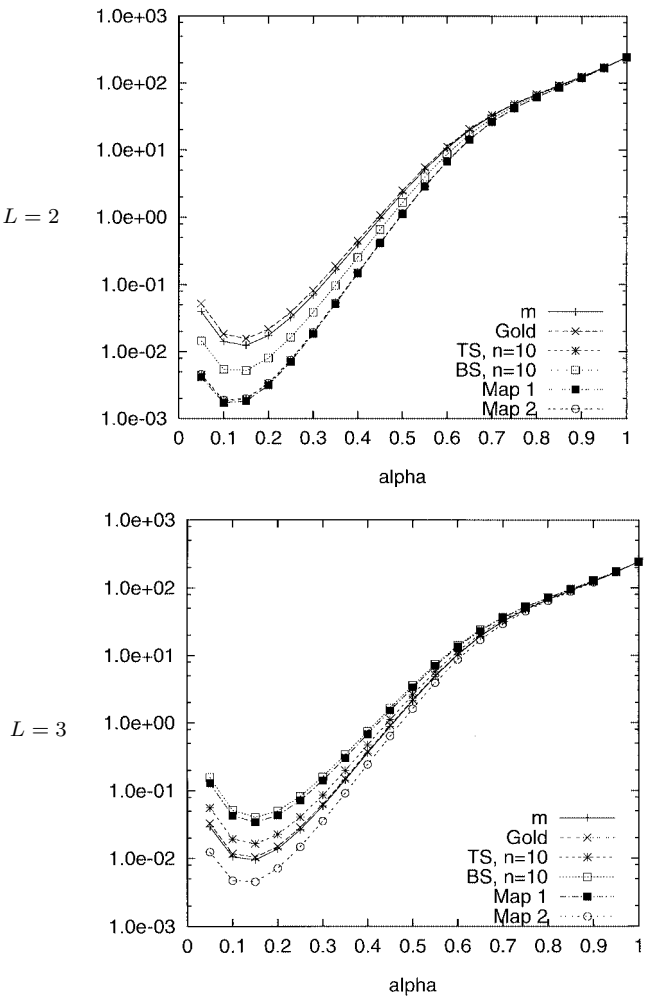

Fig. 4 Expected delay to service Ξ as a function of α for $\kappa = \eta = 2$.

It is worthwhile to notice that a typical value of $\eta = 2$ has been assumed while $\kappa = 2$ has been chosen, since it corresponds to the minimum value for Ξ in Fig. 5. Conversely, $\alpha = 0.4$ has been assumed, which do not correspond to the minimum value of Ξ in Fig. 4. In this way the considered value can be effectively employed for describing the behavior of the acquisition mechanism when thermal noise (which is unavoidable in real communication systems) is present.

Figures 7 and 8 show how T_{ac} and $\Xi = T_{ac}\Pi_o$ vary when the number of users is increased from 5 to 30 for

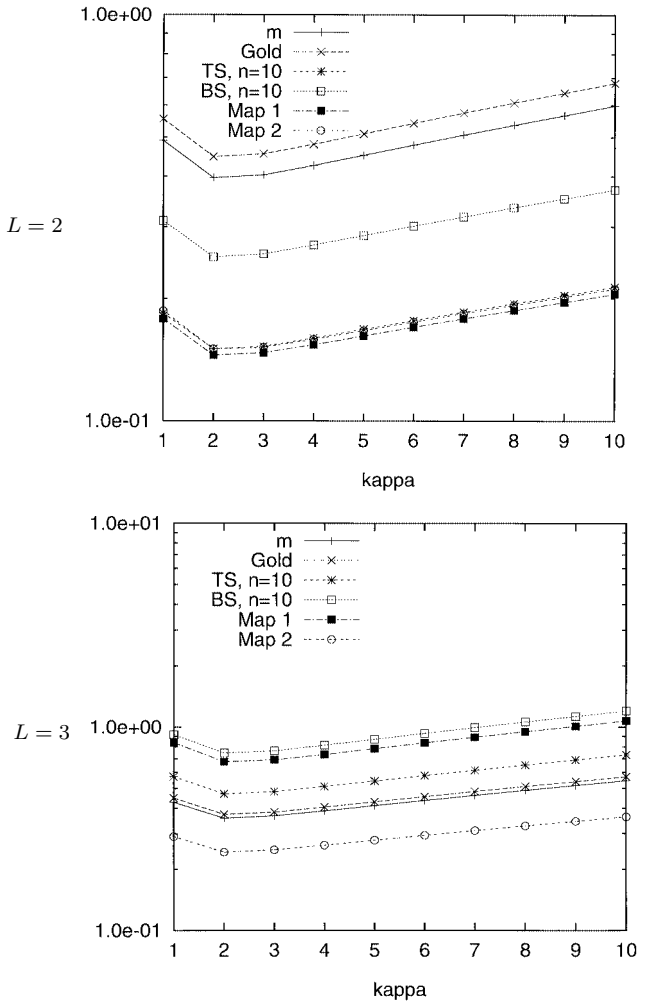

Fig. 5 Expected delay to service Ξ as a function of κ for $\alpha = 0.4$, $\eta = 2$.

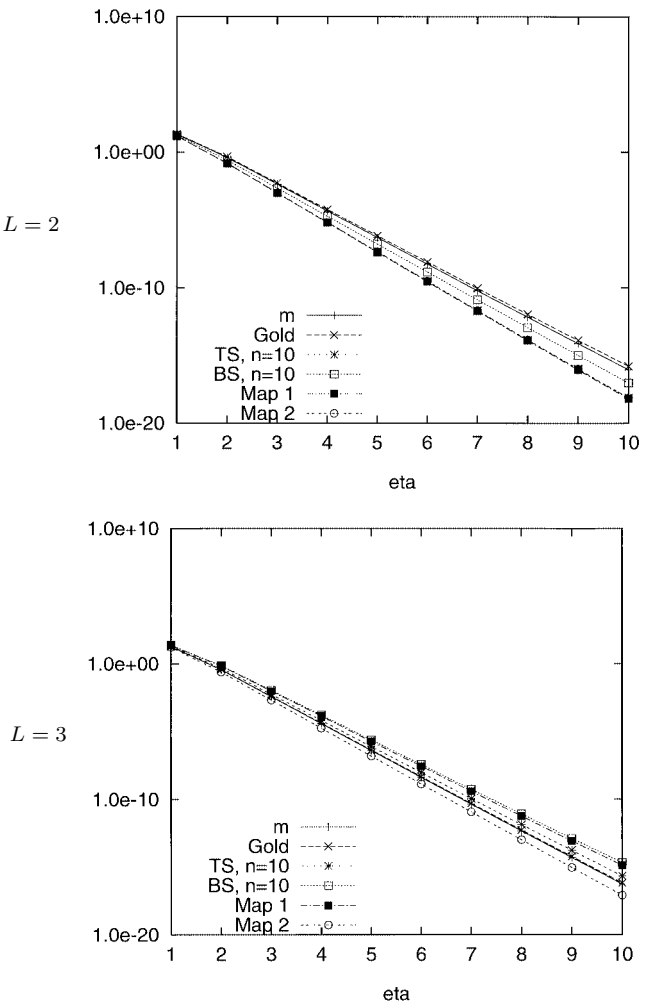

Fig. 6 Expected delay to service Ξ as a function of η for $\alpha = 0.4$, $\kappa = 2$.

$L = 2, 3, 5$. Note first that the finite T_{ac} ensures that chaos-based sequences can be synchronized though co-channel interference heavily affects overall performance which decreases as U increases. As already noted in [14], multi-level sequences result in a better average performance though chaos-based sequences exist which give rise to lower access time and outage probability. Chaos-based sequences offer better performance with respect to the classical ones in the case $L = 2$, and for all cases when sequences generated by means of Map 2 are employed.

Note that the choice $N = 70$ sets an environment in which m and Gold sequences have to be truncated and are not guaranteed to achieve their ideal performance. Yet, as the spreading factor decides the system bandwidth requirements, it is set by external considerations and can be hardly considered a degree of freedom that may be used to optimize the performance.

Nevertheless, superior performance of chaos-based spreading can be demonstrated, for example, also for $L = 2$ and $N = 127$ that allows up to $U = 18$ users adopting m-sequences and $U = 129$ users with Gold sequences, as shown in Fig. 9.

4. Conclusion

This paper deals with the influence of the adoption of chaos-based spreading sequences on the procedure of sequence phase acquisition and tracking. An improved version of the acquisition mechanism proposed in [12] is presented and thoroughly analyzed to compute the analytical expressions of suitable system performance indexes, namely outage probability, link startup delay and expected time to service. To obtain the analytical expressions of these performance merit figures, a general method is developed to derive the asymptotic state-probability of systems characterized by a given distribution of sojourn times and linked with each other by a transition graph.

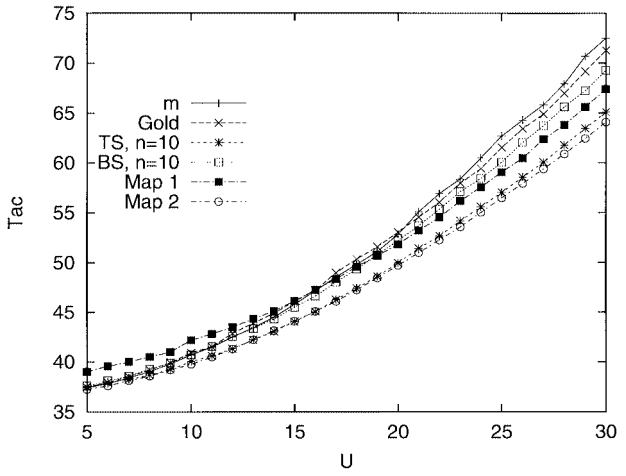

$L = 2$

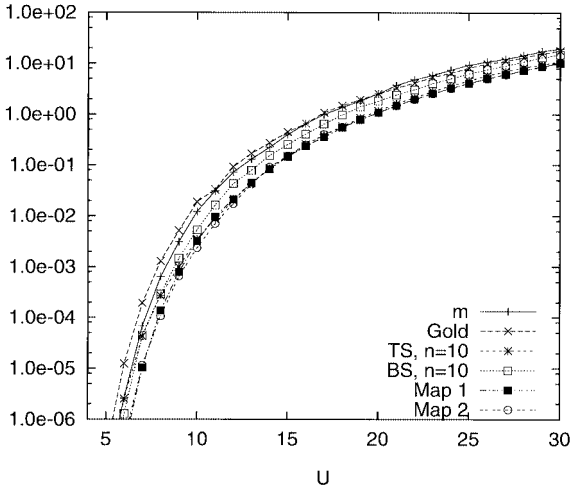

$L = 2$

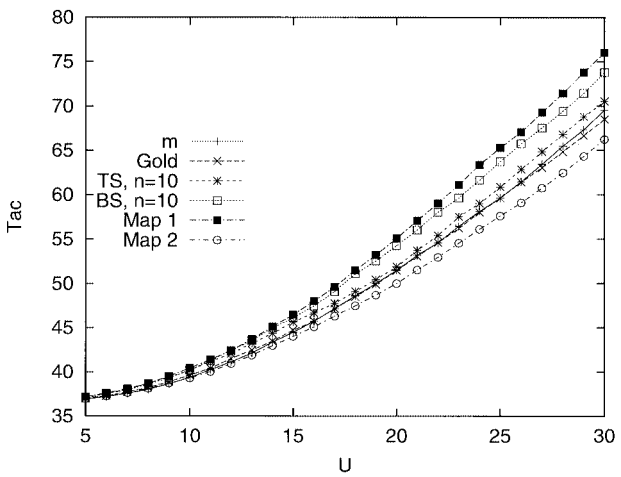

$L = 3$

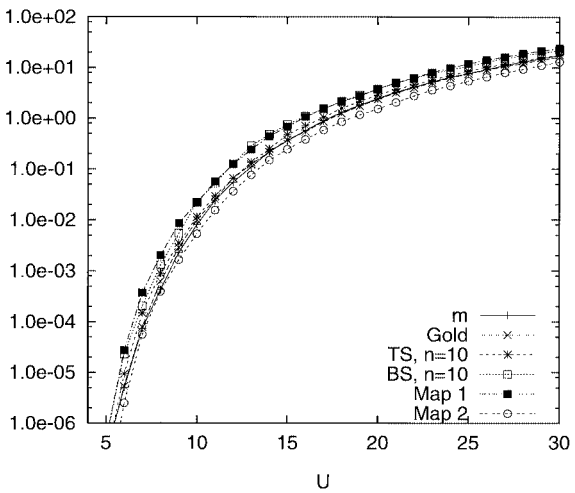

$L = 3$

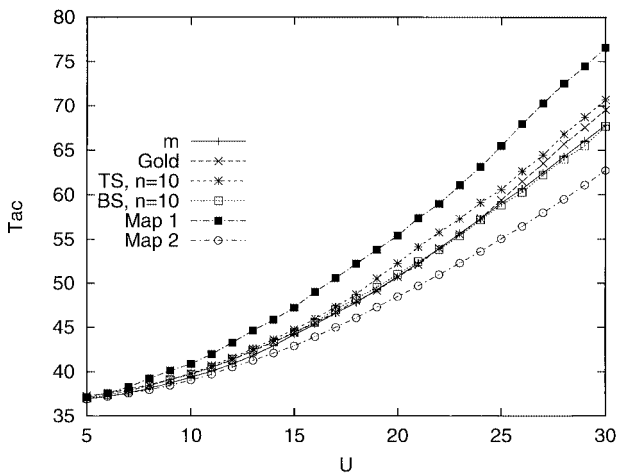

$L = 5$

Fig. 7 Access time T_{ac} as a function of U for $\alpha = 0.4$, $\kappa = \eta = 2$.

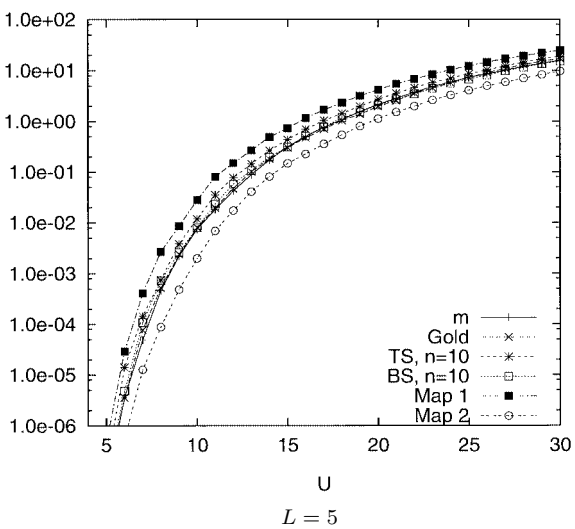

$L = 5$

Fig. 8 Expected delay to service Ξ as a function of U for $\alpha = 0.4$, $\kappa = \eta = 2$.

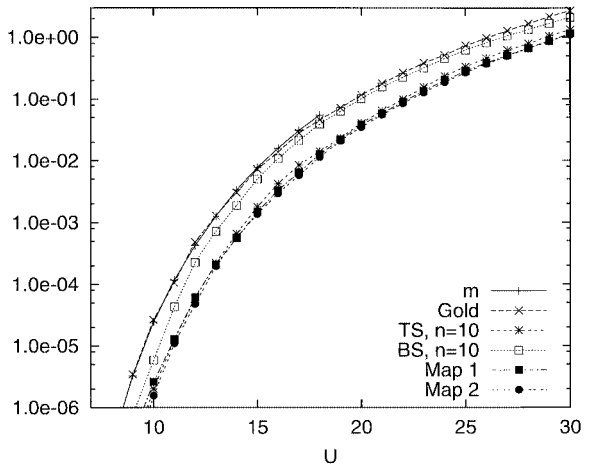

Fig. 9 Expected delay to service Ξ as a function of U for $\alpha = 0.4$, $\kappa = \eta = 2$. Comparison between chaos-based spreading and classical spreading with $N = 127$ which guarantees ideal performance for the latter.

Some new chaotic maps with respect to those employed in [12] are identified, and a first optimization phase is performed. Numerical results for the obtained optimal sequence sets are reported showing the possibility of achieving a further improvement with respect to previously reported results, and that chaotic maps exist whose generated sequences offer better performances with respect to classical ones in all the considered cases.

Several problems are still open for further investigation. For instance, the optimization procedure proposed and applied through this paper shows the possibility to select new sequences with even higher performance. Moreover, the analysis of these sequences on multi-path environment has just begun and their use in conjunction with joint detection techniques seems to be a very promising topic.

Acknowledgment

Part of this work is funded by the EC under the ESPRIT project no.31103 (INSPECT).

References

[1] G. Kolumbaán, M.P. Kennedy, and L.O. Chua, "The role of synchronization in digital communications using chaos — Part I: Fundamentals of digital communications," IEEE Trans. Circuits & Syst. — Part I, vol.44, pp.927–936, Oct. 1997.

[2] G. Kolumbán, M.P. Kennedy, and L.O. Chua, "The role of synchronization in digital communication using chaos — Part II: Chaotic modulation and chaotic synchronization," IEEE Trans. Circuits & Syst. — Part I, vol.45, Nov. 1998.

[3] G. Kolumbán, J. Schweizer, J. Ennitis, H. Dedieu, and B. Vizvári "Performance evaluation and comparison of chaos communication schemes," Proc. NDES'96, 1996.

[4] G. Kolumbán, G. Kis, Z. Jákó, and M.P. Kennedy, "FM-DCSK: A robust modulation scheme for chaotic communications," IEICE Trans. Fundamentals, vol.E81-A, no.9, pp.1798–1802, Sept. 1998.

[5] H. Dedieu and M.J. Ogorzalek, "Overview of nonlinear noise reduction algorithms for systems with known dynamics," Proc. NOLTA'98, 1998.

[6] H. Saigui, Z. Yong, H. Jandong, and B. Liu, "A synchronous CDMA system using discrete coupled-chaotic sequence," Proc. IEEE Southeastcon'96, 1996.

[7] T. Kohda and H. Tsuneda, "Even- and odd-correlation functions of chaotic chebyshev bit sequences for CDMA," Proc. IEEE International Symposium on Spread Spectrum Techniques and Applications (ISSSTA'94), 1994.

[8] G. Mazzini, G. Setti, and R. Rovatti, "Chaotic complex spreading sequences for asynchronous CDMA — Part I: System modelling and results," IEEE Trans. Circuits & Syst. I, vol.44, no.10, pp.937–947, 1997.

[9] R. Rovatti, G. Setti, and G. Mazzini, "Chaotic complex spreading sequences for asynchronous CDMA — Part II: Some theoretical performance bounds," IEEE Trans. Circuits & Syst. I, vol.45, no.4, pp.496–506, 1998.

[10] R. Rovatti and G. Mazzini, "Interference in DS-CDMA systems with exponentially vanishing autocorrelations: Chaos-based spreading is optimal," IEE Electron. Lett., vol.34, pp.1911–1913, 1998.

[11] A.J. Viterbi, CDMA, Addison-Wesley, 1995.

[12] G. Mazzini, R. Rovatti, and G. Setti, "Sequence synchronization in chaos-based DS-CDMA systems," Proc. ISCAS '98, 1998.

[13] H. Minc, Nonnegative Matrices, Wiley - Interscience, 1987.

[14] G. Mazzini, "Analytical formulation for the synchronization performance of Q-level M-sequences in DS-CDMA," Proc. GLOBECOM'94, 1994.

[15] G. Setti, G. Mazzini, and R. Rovatti, "Gaussian characterization of self-interference during synchronization of chaos based DS-CDMA systems," Proc. ICECS'98, 1998.

[16] R. Rovatti, G. Setti, and G. Mazzini, "Statistical features of chaotic maps related to CDMA systems performance," Proc. MTNS'98, 1998.

[17] G. Mazzini, "DS-CDMA systems using q-level m sequences: Coding map theory," IEEE Trans. Commun., vol.45, pp.1304–1313, 1997.

Appendix

Here, a general method is developed to derive the steady-state probability of a given mode of operation for a system characterized by M modes. The time t_i in which the system maintains the i-th mode is random and has a given distribution

$$\mathcal{F}_i(k) = \Pr\{t_i > k\} \qquad (\mathrm{A}\cdot 1)$$

while, once the system exits the i-th mode, it has a given probability Π_{ij} of entering the j-th mode. The corresponding transition graph is reported in Fig. A· 1.

From (A· 1) with $k = 1, 2, \ldots$ and $\mathcal{F}_i(0) = 1$, one can derive the steady state probability Σ_i associated to each mode of the system.

Theorem 1: If the transition probability matrix $\bar{\Pi} = [\Pi_{ij}]$ is irreducible and the distribution of sojourn times $\mathcal{F}_i(k)$ is such that

$$\mathcal{G}_i = \sum_{k=0}^{\infty} \mathcal{F}_i(k) < \infty \qquad (\mathrm{A}\cdot 2)$$

then the steady state values of the system mode probabilities are expressed by

$$\Sigma_i = \frac{\pi_i \mathcal{G}_i}{\sum_{j=0}^{M-1} \pi_j \mathcal{G}_j} \quad i = 0, \ldots, M-1 \qquad (\text{A}\cdot 3)$$

where $\pi = [\pi_i]$ is the unique eigenvector corresponding to the unit eigenvalue of $\bar{\Pi}$.

Proof: Starting from the system transition graph, it is possible to construct an infinite Markov chain whose states can be partitioned in M subsets such that the sojourn time in the i-th subset is regulated by $\mathcal{F}_i(k)$. To do this, substitute each mode in the transition graph of Fig. A· 1 with a infinite chain as shown in Fig. A· 2. In particular, $p_{i,k} = \mathcal{F}_i(k+1)/\mathcal{F}_i(k)$ is the transition probability from state k to state $k+1$ in the infinite chain associated to mode i in the original system, while $q_{i,k,j} = (1-p_{i,k})\Pi_{ij}$ represents the probability of evolution from state k associated to mode i to the first state of the chain corresponding to mode j.

Such a infinite state Markov chain can be exploited to compute Σ_i. To this aim, note first that due to the particular structure of each chain, and since $\bar{\Pi}$ is irreducible, every state can be reached by any other state in finite time. Hence, the Markov chain is ergodic and a unique steady-state probability $\sigma_{i,k}$ exists associated to each state k corresponding to mode i. For $k > 0$ this invariant probability assignment must be such that

$$\begin{aligned}\sigma_{i,k} &= p_{i,k-1}\sigma_{i,k-1} \\ &= \prod_{l=1}^{k} \frac{\mathcal{F}_i(l)}{\mathcal{F}_i(l-1)}\sigma_{i,0} \\ &= \mathcal{F}_i(k)\sigma_{i,0} \end{aligned} \qquad (\text{A}\cdot 4)$$

while, by using (A· 4) one has

$$\begin{aligned}\sigma_{i,0} &= \sum_{j=0, j\neq i}^{M-1} \sum_{k=0}^{\infty} q_{j,k,i}\sigma_{j,k} \\ &= \sum_{j=0, j\neq i}^{M-1} \sum_{k=0}^{\infty} \left(1 - \frac{\mathcal{F}_j(k+1)}{\mathcal{F}_j(k)}\right) \Pi_{ji}\mathcal{F}_j(k)\sigma_{j,0} \\ &= \sum_{j=0, j\neq i}^{M-1} \Pi_{ji}\sigma_{j,0} \end{aligned} \qquad (\text{A}\cdot 5)$$

where the last equality holds since $\mathcal{F}_j(0) = 1$ and from (A· 2) we get $\mathcal{F}_i(k) \to 0$ when $k \to \infty$. As $\bar{\Pi}$ is associated to a pure transition graph, $\Pi_{ii} = 0$ for any i and thus Eq. (A· 5) implies that $\sigma_{i,0} = \beta\pi_i$, where $\pi = [\pi_i]$ is the eigenvector corresponding to the unit eigenvalue of $\bar{\Pi}$, which is unique since $\bar{\Pi}$ is a non-negative irreducible matrix [13], and thus the original system is ergodic. The positive constant β must be chosen to satisfy the normalization condition

$$\sum_{i=0}^{M-1} \sum_{k=0}^{\infty} \sigma_{i,k} = 1 \qquad (\text{A}\cdot 6)$$

so that, by using (A· 4), one gets $\beta \sum_{i=0}^{M-1} \pi_i \sum_{k=0}^{\infty} \mathcal{F}_i(k) = 1$ which results in $\beta = \left(\sum_{i=0}^{M-1} \pi_i \mathcal{G}_i\right)^{-1}$. With this, the probability of being in mode i in the original system can be expressed as $\Sigma_i = \sum_{k=0}^{\infty} \sigma_{i,k} = \sigma_{i,0} \sum_{k=0}^{\infty} \mathcal{F}_i(k) = \pi_i \mathcal{G}_i \left(\sum_{j=0}^{M-1} \pi_j \mathcal{G}_j\right)^{-1}$. □

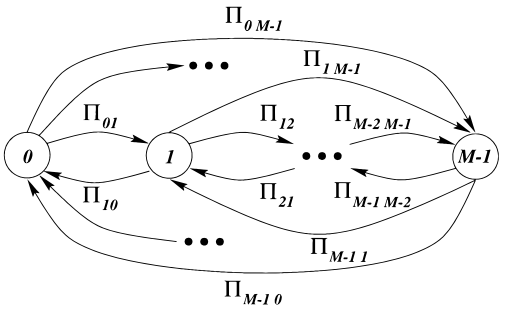

Fig. A· 1 Transition graph of a system with M modes of operation and characterized by a transition probability matrix $\bar{\Pi}$.

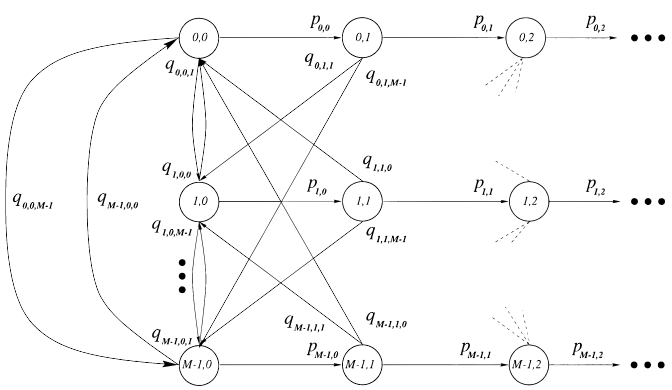

Fig. A· 2 Transition graph of the infinite Markov chain characterized by the same distribution of sojourn times as the original system with transition graph shown in Fig. A· 1.

To complete the set of tools needed to derive the merit figures of the synchronization mechanism proposed in Sect. 2, note that $\mathcal{G}_i$ represents the expected system permanency time in mode i. In fact, if $f_i(k)$ indicates the probability that the system stays in mode i exactly k time steps, one has $\mathcal{F}_i(k) = \sum_{j=k+1}^{\infty} f_i(j)$, and therefore

$$\begin{aligned}\mathcal{G}_i &= \sum_{k=0}^{\infty} \sum_{j=k+1}^{\infty} f_i(j) \\ &= \sum_{l=1}^{\infty} l f_i(l). \end{aligned} \tag{A·7}$$

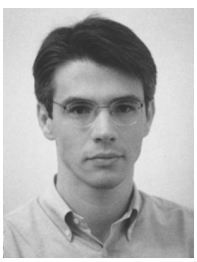

Gianluca Setti was born in Modena, Italy, on September 13, 1965. He received the Dr. Eng. degree (with honors) in Electronic Engineering and Ph.D. degree in Electronic Engineering and Computer Science from the University of Bologna, Bologna in 1992 and 1997, respectively. From May 1994 to July 1995 he was with the Circuits and Systems Group of the Swiss Federal Institute of Technology as visiting Ph.D. student. In 1998 he received the Caianiello prize for the best Italian Ph.D. thesis on Neural Networks. Since 1997 is has been a Lecturer and since 1998 he is a assistant professor of Analog Electronics at the University of Ferrara. His research interests include nonlinear circuit theory, recurrent neural networks, and the design, implementation, and applications of chaotic circuits and systems. Dr. Setti is currently serving as an associate editor of the IEEE Transactions on Circuits and Systems – Part I. E-mail:gsetti@ing.unife.it

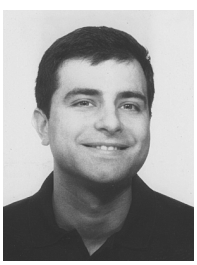

Riccardo Rovatti was born in Bologna, Italy, on January 14, 1969. He received the Dr. Eng. degree (with honors) in Electronic Engineering and Ph.D. degree in Electronic Engineering and Computer Science from the University of Bologna, Bologna in 1992 and 1996, respectively. Since 1997 he is a lecturer of Digital Electronics at the University of Bologna. He authored or co-authored more than sixty international scientific publications. His research interest include fuzzy theory foundations, learning and CAD algorithms for fuzzy and neural systems, statistical pattern recognition, function approximation, non-linear system theory and identification as well as applications of chaotic systems. E-mail:rrovatti@deis.unibo.it

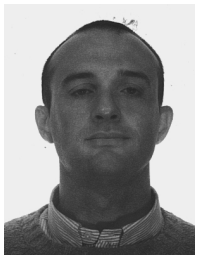

Gianluca Mazzini was born in Bologna, Italy, on January 3, 1968. He received the Dr. Eng. degree (with honors) in Electronic Engineering and Ph.D. degree in Electronic Engineering and Computer Science from the University of Bologna, Bologna in 1992 and 1996, respectively. Since 1996 he has joined the University of Ferrara where he is an assistant professor of Telecommunications Networks. His research interests are related to spread spectrum communications, chaos based communication systems, Internet mobile computing, cellular handover procedures and protocols for wireless local area networks. E-mail:gmazzini@ing.unife.it